

# **LEGIBILITY NOTICE**

A major purpose of the Technical Information Center is to provide the broadest dissemination possible of information contained in DOE's Research and Development Reports to business, industry, the academic community, and federal, state and local governments.

Although a small portion of this report is not reproducible, it is being made available to expedite the availability of information on the research discussed herein.

DEC 04 1989

Los Alamos National Laboratory is operated by the University of California for the United States Department of Energy under contract W-7405-ENG-36

LA-UR--89-3767

DE90 003395

TITLE: PROGRESS WITH SMALL, HIGH MAGNETIC FIELD SPHEROMAKS IN CTK

AUTHOR(S): WYSOCKI, F.J., CTR-5  
FERNANDEZ, J.C., CTR-5  
HENINS, I., CTR-5  
\*JARBOE, T.R., University of Washington  
\*(work performed while at CTR-5)  
MARKLIN, G.J., CTR-6  
MAYO, R.M., CTR-5

SUBMITTED TO Submitted to the US/Japan Compact Toroid Workshop held November 6-9, 1989 at Los Alamos National Laboratory

DISCLAIMER

This report was prepared as an account of work sponsored by an agency of the United States Government. Neither the United States Government nor any agency thereof, nor any of their employees, makes any warranty, express or implied, or assumes any legal liability or responsibility for the accuracy, completeness, or usefulness of any information, apparatus, product, or process disclosed, or represents that its use would not infringe privately owned rights. Reference herein to any specific commercial product, process, or service by trade name, trademark, manufacturer, or otherwise does not necessarily constitute or imply its endorsement, recommendation, or favoring by the United States Government or any agency thereof. The views and opinions of authors expressed herein do not necessarily state or reflect those of the United States Government or any agency thereof.

DISTRIBUTION OF THIS DOCUMENT IS UNLIMITED

By acceptance of this article the publisher recognizes that the U.S. Government retains a nonexclusive, royalty-free license to publish or reproduce the published form of this contribution or to allow others to do so for U.S. Government purposes.

The Los Alamos National Laboratory requests that the publisher identify this article as work performed under the auspices of the U.S. Department of Energy.

MASTER



Los Alamos Los Alamos National Laboratory  
Los Alamos, New Mexico 87545

## Progress with Small, High-Magnetic-Field Spheromaks in CTX\*

F. J. Wysocki, J. C. Fernández, I. Henins,  
T. R. Jarboe<sup>†</sup>, G. J. Marklin, and R. M. Mayo

Los Alamos National Laboratory,  
Los Alamos, NM 87545

### INTRODUCTION

The current CTX program is directed towards using spheromaks as an energy transfer medium to accelerate metal plates to hypervelocity. In the proposed scheme, the spheromak is first compressed by accelerating a large plate to moderate velocity (3 – 5 km/s) with high explosives (HE). Another smaller plate is designed such that it experiences little force until the spheromak is compressed to a size comparable to the small plate. Then the force on the small plate rises quickly, accelerating this plate to high velocity. Figure 1 shows the present design for a proof-of-principle experiment. Present theoretical calculations indicate velocity gain of the small plate over the large plate as high as four (geometry not the same as Fig. 1), which could produce 20 km/s small plate velocity. In principle, the final velocity is limited only by the sound speed of the spheromak (which is very high), and in practice, is probably limited by ohmic heating in the plate (leading to melting), the amount of energy that can be delivered to the large compression plate, and the energy dissipated by the spheromak during compression. Taking these effects into account, final velocities in the range 40 – 100 km/s might be achievable.

Final velocities approaching 100 km/s will require compressed spheromak energy densities comparable to that of HE ( $B \approx 100$  T). The desire to keep the quantity of compression HE down to moderate levels (of order 100 pounds) dictates small initial spheromak size ( $\lesssim 0.3 - 0.4$  m). Thus, it is necessary to be able to produce small spheromaks with as high an initial magnetic field strength as possible. A proof-of-principle, velocity gain greater than one, experiment probably requires the initial maximum internal spheromak field to be  $\gtrsim 3$  T, and future experiments may require  $\gtrsim 10$  T. In addition, the spheromak magnetic energy dissipated during compression should be minimized. Although compression times of 80 – 100  $\mu$ s are short compared to magnetic decay times in large (0.5 – 1 m) spheromaks, the decay time drops as the spheromak is compressed to small size. Thus, it is desirable to have the spheromak

as hot as possible, and any “anomalous” resistivity should be minimized. Figure 2 shows the expected velocity gain as a function of both the initial maximum internal magnetic field and the initial magnetic decay time, for the geometry shown in Fig. 1.

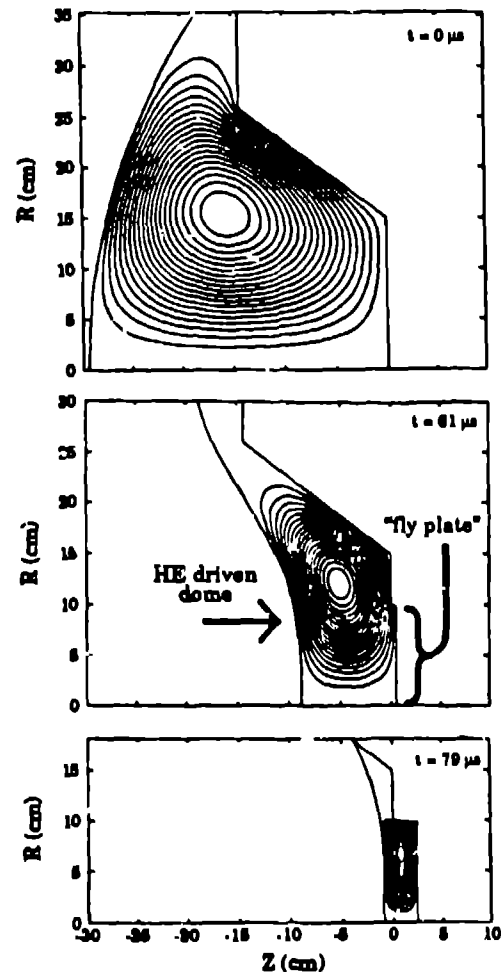


Figure 1: Numerical simulation of spheromak dynamics in the presence of a compressing dome. The “fly plate” is the small plate that is accelerated (starting at  $\approx 79 \mu$ s) to hypervelocity. Spheromak resistive decay is included in this simulation.

The CTX facility is being used to develop needed techniques to produce small, high-field, low-resistance spheromaks in the laboratory. This will soon include testing a new plasma gun which is inexpensive enough to eventually “blow up” at an HE firing site. The present experiments use the same gun which was used for the 0.67-m mesh flux conserver and the 0.61-m solid-wall flux conserver experiments. Figure 3 shows the new solid-wall low-magnetic-field-error flux conserver that has been installed with both radius and length equal to 0.28-m,

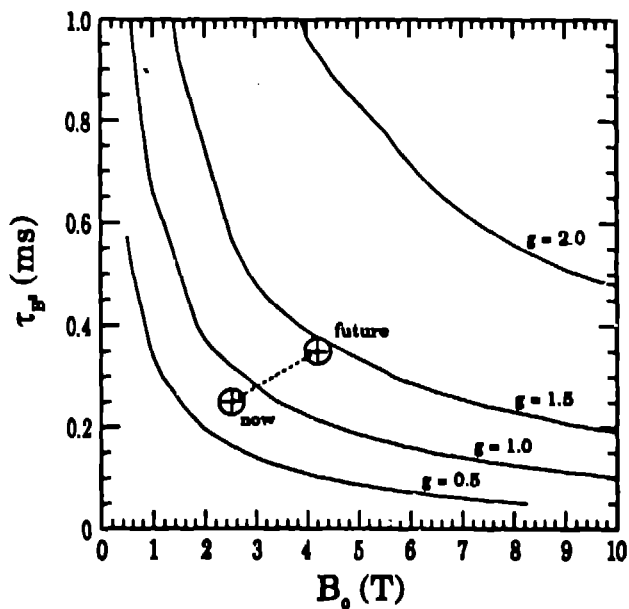


Figure 2: Required initial decay time vs. initial internal spheromak magnetic field for velocity gain of 0.5, 1.0, 1.5, and 2.0. The dashed line connects the point of present spheromak parameters with that we expect in the near future.

which is equal to the outer-electrode radius of the gun. The inter-electrode spacing is no longer a small perturbation on the spheromak. The advantage of this arrangement is the increased energy efficiency of the gun due to better  $\lambda$  matching of the gun and the spheromak. In addition, the external capacitor bank circuit has been changed to give shorter ( $\approx 180 \mu\text{s}$ ), higher-powered pulses to the plasma gun.

## RESULTS

The highest maximum internal field obtained to date is  $\approx 3.5 \text{ T}$ , but the majority of the data obtained thus far is from spheromaks with  $\approx 2.2 - 2.6 \text{ T}$  maximum internal field. The longest spheromak lifetime is  $\approx 1 \text{ ms}$  for these conditions. Thomson scattering electron temperature profiles show  $T_e$  as high as  $350 - 400 \text{ eV}$ . (Ability to measure still higher temperatures requires a modification to the Thomson scattering spectrometer, which is currently underway.)

In many figures in this report, reference is made to the value  $B_3$  (measured by the four magnetic probes at position #3 separated by  $90^\circ$  toroidally, see Fig. 3). For reference, the maximum internal field is roughly 2.2 times as great as  $B_3$ , and  $1 \text{ MA}$  of toroidal plasma current produces  $1.3 \text{ T}$  for  $B_3$ .

Several interesting types of spheromak behavior have been observed in this flux conserver. The

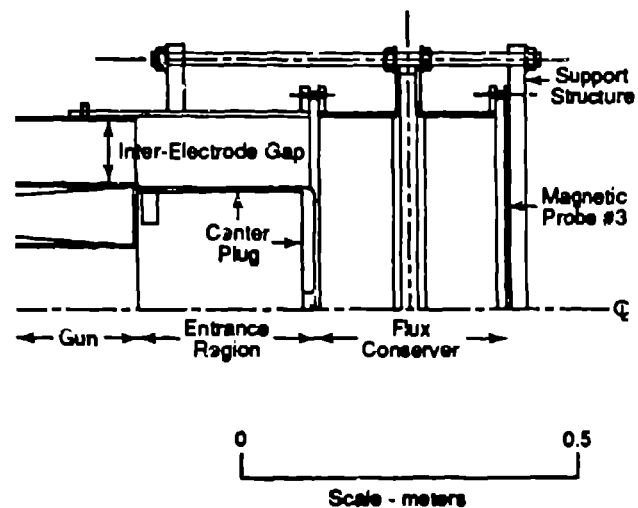


Figure 3: This figure shows the present small flux conserver used in CTX (made of OFHC copper). Also indicated are the end of the plasma gun, the entrance region and associated center plug (both made of OFHC copper), the magnetic probes (seven positions indicated, each with 4 probes separated by  $90^\circ$  toroidally), and the support structure. The magnetic pressure developed in present spheromaks was causing the flux conserver to crack. The support structure (made of 304SS) was installed to prevent cracking. The position of the probes which give the  $B_3$  data referred to in the text is indicated.

spheromak tends to  $n=1$  tilt (or kink) globally into the entrance region after sustainment, which has not been observed before in CTX. This is related to the fact that the flux conserver diameter is now exactly the same as the gun and entrance region diameters. Fortunately, this tendency is substantially reduced for the hotter spheromaks obtained, as shown in Fig. 4. Another observation is the degradation of energy and particle confinement times, which is associated with the standard  $n=2$  kink mode present during decay of hot spheromaks, shown in Fig. 5. While this phenomenon was previously observed in the mesh-walled flux conserver, the degradation was attributed to the large magnetic field errors. The  $n=2$  kink mode had no apparent degradation on discharges in the 0.61-in solid-wall flux conserver, which used a low-field-error design. The present flux conserver also has a solid wall and is designed to have few field errors. The new data indicate a source of field errors that was not anticipated. Possibilities include the entrance region, which is perforated with  $1''$  diameter holes,  $2''$  center to center (for historical

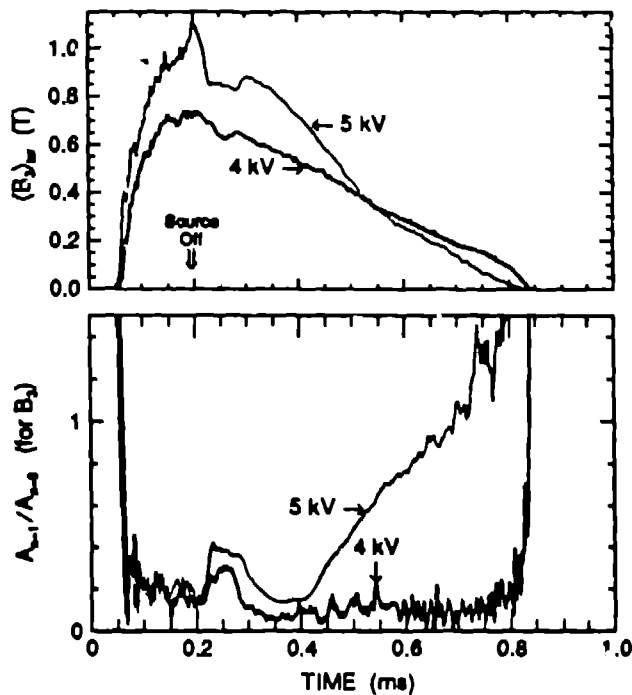


Figure 4: This data indicates the behavior of the  $n=1$  distortion which is frequently observed after sustainment for two sequential discharges. The quantity  $A_{n=1}/A_{n=0}$  represents the ratio of the amplitudes for the  $n=1$  distortion to the axisymmetric state, as determined by the  $B_3$  data (see Fig. 3). Notice the growth and decay of the mode between  $t = 0.2$  to  $t \approx 0.3$  ms in both discharges, however only the 5 kV discharge distorts starting at  $t = 0.4$  ms (the voltage refers to the capacitor bank voltage for the gun). Thomson scattering data at  $t = 0.41$  ms indicates that the 4 kV discharge had central electron temperature and density of 145 eV and  $1.8 \times 10^{14} \text{ cm}^{-3}$ , while the 5 kV discharge had only 48 eV and  $5.6 \times 10^{14} \text{ cm}^{-3}$ . While hot discharges without  $n=1$  distortions have been produced at 5 kV (see Fig. 5 for example), there tends to be strong  $n=1$  distortion for colder discharges regardless of bank voltage.

reasons), rounded corners with too small a radius of curvature leading to flux penetration, and the fact that the flux conserver is (unfortunately) distorted and out-of-round. Additionally, the comparatively large inter-electrode spacing may make the  $n=2$  kink mode intrinsically more detrimental. An effort to understand this situation is ongoing.

The data in Figs. 6 - 8 summarize some of the best results obtained in the latest configuration. The line average density is obtained from the  $\text{CO}_2$  interfer-

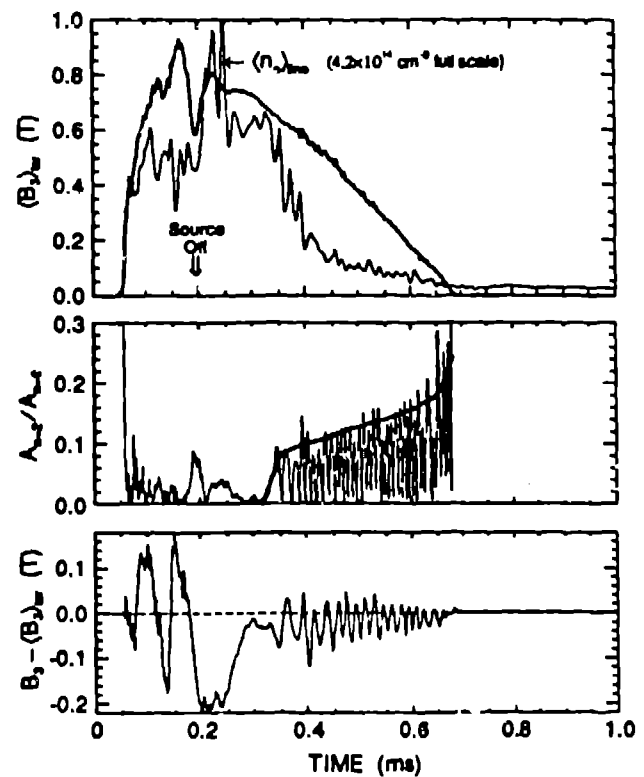


Figure 5: This data indicates the degradation of particle and energy confinement times correlated with  $n=2$  activity normally present during decay of hotter discharges. The quantity  $A_{n=2}/A_{n=0}$  represents the ratio of the amplitudes for the  $n=2$  mode to the axisymmetric state, as determined by the  $B_3$  data (see Fig. 3). The fast oscillatory behavior after  $t = 0.34$  ms is an artifact of the simplistic technique used to obtain  $A_{n=2}$ ; the real value is the envelope, as indicated by the heavy line. Notice the "pump out" of plasma density starting as soon as the  $n=2$  activity starts, and the increased decay rate of  $B_3$  starting  $\approx 0.08$  ms later. The detriment is believed to be caused by unexpected magnetic field errors.

ometer, and the Thomson scattering data is from the multi-point system, which covers an entire radius of the flux conserver, and is absolutely calibrated for density using Raman scattering in nitrogen.

#### ACKNOWLEDGMENTS

The authors acknowledge the expert technical assistance of Robert Bollman, Richard Scarberry, and Dennis Martinez.

\* Work supported by Los Alamos National Laboratory Internal Scientific Research funds.

† Present Address: University of Washington, Seattle, WA 98195

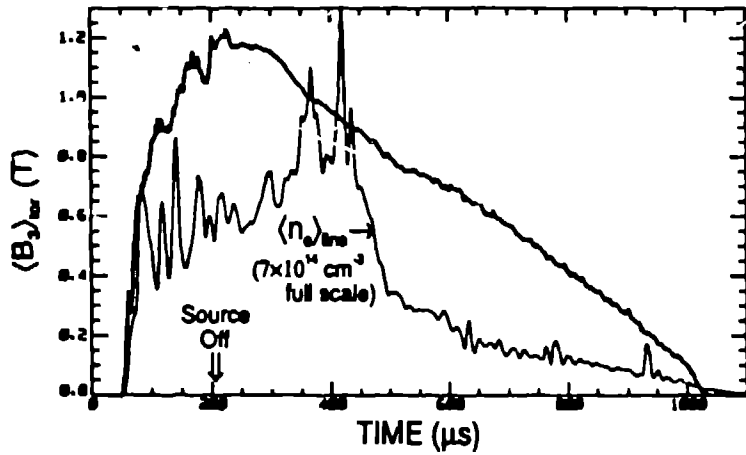


Fig. 6. This figure shows a long lived, high field discharge. The highest field produced at present is 1.6 T wall field, but these discharges are not yet optimized, and therefore do not last as long.

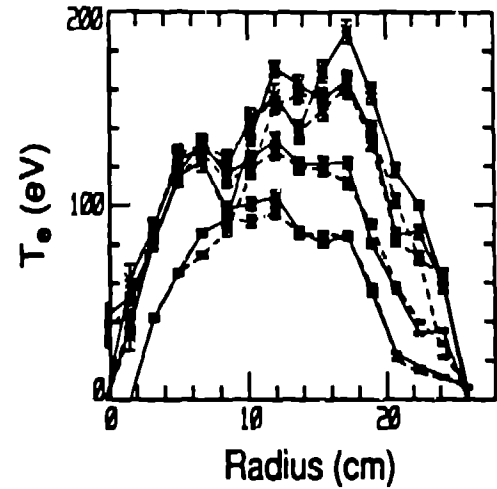


Fig. 7. This figure shows the Thomson scattering data at 260 μs from four discharges with 1.0 T maximum wall field and  $\approx 6 \times 10^{14}$  density at the laser firing time.

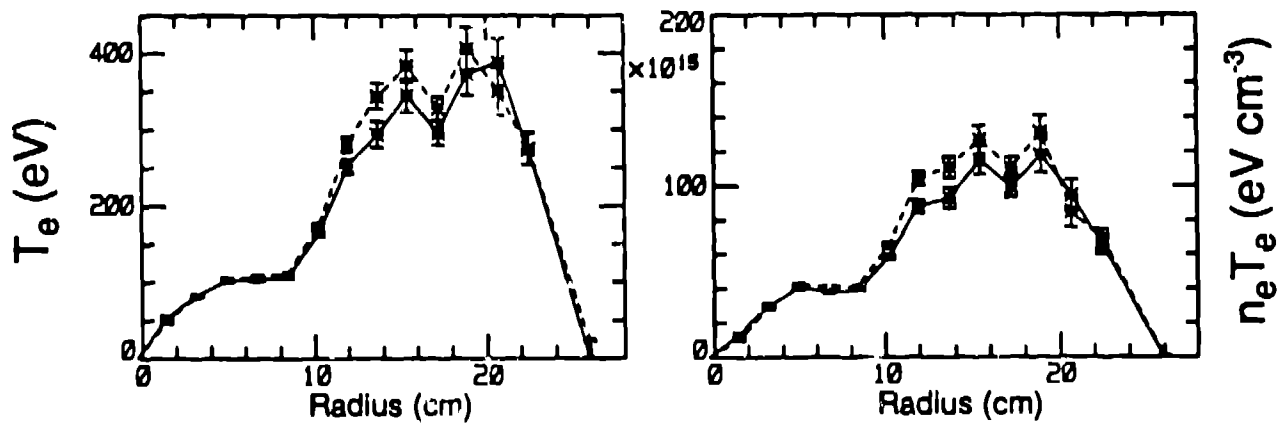
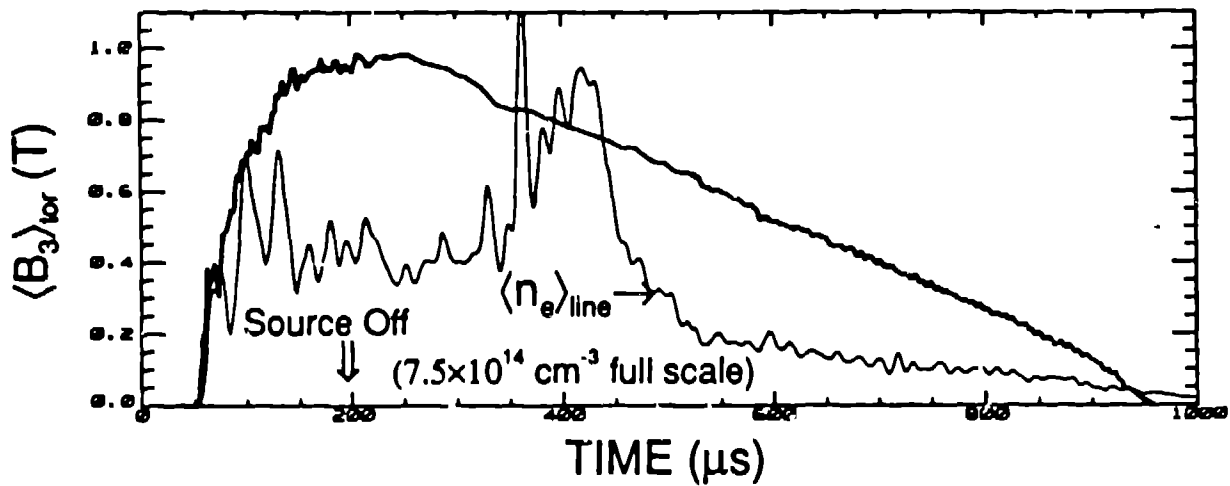


Fig. 8. This figure shows the wall field and density vs time, and the Thomson scattering data at 310 μs for one of several discharges with data above 200 eV.